



Reservoir characterization of Roncador, Campos Basin

Carlos Rodriguez-Suarez*, Jorge André B. de Souza, Darci J. Sarzenski, Mauro Ida and Vera Lúcia G. Elias
PETROBRAS/UN-RIO/ATP-RO/RES

Copyright 2003, SBGf - Sociedade Brasileira de Geofísica

This paper was prepared for presentation at the 8th International Congress of The Brazilian Geophysical Society held in Rio de Janeiro, Brazil, 14-18 September 2003.

Contents of this paper was reviewed by The Technical Committee of The 8th International Congress of The Brazilian Geophysical Society and does not necessarily represents any position of the SBGf, its officers or members. Electronic reproduction, or storage of any part of this paper for commercial purposes without the written consent of The Brazilian Geophysical Society is prohibited.

Abstract

Roncador field, at Campos Basin, is characterized by the presence of several compartments with distinct hydrocarbon API grades and fluid contacts. Geologic modeling used in flow simulation involved the determination of the spatial distribution of key reservoir petrophysical properties, interpolated between wells, constrained by seismic data. Modeling results suggest a dominant depositional control of petrophysical properties. Despite the encouraging results, some questions related to blocks and reservoir connections and reservoir heterogeneities are yet to be answered.

Roncador field: geological aspects

Roncador field is located 130 Km offshore Brazilian southeastern coast and produces 90,000 b/d from sandstone reservoirs at 1,500-1,900 m water depths (the sea floor is a smooth, easterly dipping surface) (Fig.1 and 3).

The reservoirs are thick (up to 300 m), excellent quality ($\phi = 27-30\%$; $k = 200-4,000$ mD) dominantly massive, turbidite sandstones of Maastrichtian age, interbedded with shales and marls. The trap is of structural/stratigraphic type.

The field is composed by two main blocks, separated by a NW-SE normal fault (RF-Roncador Fault; maximum throw of 200 m, dipping E-NE) and has been divided into four modules (Fig. 2). Module M1, in the hanging wall, is located on the eastern and northern parts, being characterized by the occurrence of 27-31^o API oil. The other domain, in the footwall, includes Modules M2, M3 and M4 and is the focus of this work. M2 (drilled by wells A, G and H) and M4 (wells B and E) have 18^o oil, whereas M3 reservoirs are filled with 22^o API oil. The different oil-type compartments in the footwall domain are separated by a N-S discontinuous normal fault zone dipping eastwards at high angles. Multiple gas-oil (GOC) and oil-water (OWC) contacts occur at Roncador. Total reserves for M2, M3 and M4 are estimated in 1.3 .10⁹ BOE.

The main footwall reservoirs, at depths of 2,700 to 3,300 m, are limited east and north by faulting, and to west and south by pinch. They occur within a quaquaversal-type structure. Main complexities for reservoir characterization are oil type and tectonic framework, with most of the

faulting being associated with movements of Aptian salt bodies (750 to 2,100 m below reservoir base).

On a semi-detail seismic section crossing all wells, depositional and tectonic features as erosive surfaces and faults actives at different ages can be identified. The reservoir dips gently towards E-SE and is dominated by the presence of steep normal fault zones (kink zones) with throws (range of few cm to 10-40 m) much smaller than the reservoir thickness (100-250 m) (Fig. 3).

Reservoir lithologies are dominated by arkosic sandstones of Upper Maastrichtian age, divided into several production zones; the most important zone (330) is subdivided into 330A, 330B and 330C. The general depositional framework involves more proximal, channel deposits composed by amalgamated, coarse- to medium-grained massive sands with erosive bases, overlain by more widespread, tabular sandstone lobes, with fine-grained, thin-bedded turbidites at the top.

Seismic aspects of Roncador

The field is covered by two 3D seismic data, acquired in 1992 and 1999; both 3D were acquired E-W and had Kirchhoff PSTM applied on them, using an algorithm developed and applied by PETROBRAS (Rosa *et al.*, 1999).

Seismically, reservoir tops are characterized by an acoustic impedance decrease. The base is defined mainly by an erosive surface; at four wells (B, E, G and H), the base shows a decrease in impedance, whereas the opposite is observed for the other wells. 330C top is characterized on logs and seismic by a decrease on impedance. No impedance contrast occurs for 330B top – for this reason, this surface was mapped using an erosion close to 330A/B boundary. The erosion pattern along the reservoir base is clearer when the top is flattened (Fig. 4). Results of acoustic inversions were considered superior to conventional seismic data, with better discrimination and continuity of events considered representative of geologic events (Fig. 4). The inversion generated data with phase slightly different from the original, and, as the data quality did not allow an automatic correction, the whole interpretation had to be redone manually.

Two different algorithms, one proprietary and another commercial, were used for inversion. The in-house method (Rosa and Tassini, 1995) applies a non-stationary wavelet, but does not use geologic model constraints, neither recovers low frequencies from well logs (these are obtained from seismic velocities). The commercial software uses a model-based inversion, using a stationary wavelet (obtained by averaging well-seismic ties). Both results were converted to depth using a proprietary image-ray based method (Filpo and Zago, 2001). Two elastic inversion approaches (one proprietary, based on Moraes (2000), and the other commercial) were

tested in the 1992 data, but the results were not good, mainly due to poor S/N on the far offsets; both techniques will be tested in the seismic data acquired in 1999.

Analysis of coherence data confirmed the structural interpretation done on vertical seismic sections. This interpretation showed a quaquaversal structure with its apex at center-west of the area (Fig. 5). Three main structural patterns can be inferred, two orthogonal (N-S and E-W) and a ring-type around the structure apex.

Engineering aspects of Roncador

Drill stem tests (DSTs) on wells B and D helped reservoir characterization regarding presence of faults, permeability information and productivity index – all of them fundamental for the development plan. Data on production flow and pressures and temperatures on bottom (PDG) and surface (TPT) were obtained from an extended testing on well D; these information were used on flow simulation to check the geologic model, reservoir compartmentalization, semi-barrier faults and vertical reservoir communication. As a match between static and dynamic models was obtained, cost and uncertainty reduction and optimization for the exploitation final plan were possible. Another extended well test is planned for the first horizontal well to be drilled in the footwall; the static (geologic) model will be checked with information from this test.

Appraisal wells

Well F was drilled with the aim to better define the northern limit between M3 and M4. Its location was defined using acoustic inverted seismic data, neural network and indications of a possible OWC (on depth converted data) (Rodriguez-Suarez, 2002).

Wells G and H were drilled to 1) determine oil viscosity, 2) add proven hydrocarbon reserves in the southwestern part of the field, 3) confirm the existence of 330C, a conglomerate-rich zone which is an excellent reservoir, 4) be used as pilot to horizontal wells, 5) refine the geological model, and 6) verify possible OWCs not seen in seismic data. All purposes have been met for both wells. Well G found reservoir 50 m thicker than expected, due to a conservative interpretation for the reservoir bottom.

Petrophysical parameters from seismic attributes

Besides the seismic attributes commonly used in reservoir characterization (e.g., complex attributes and amplitude), two additional attributes were tested (and used) on this study. One is defined by the terms of a polynomial that reconstructs the seismic traces; the other, the difference (error) between the hypothetical reconstructed trace using each individual term alone and the actual seismic trace. All attributes used represent an average for the top-to-bottom reservoir (or layer) interval. During the verification of the correlation between seismic attributes and petrophysical parameters, the analyses were performed separately for two groups, one including M2 and M4 and the other for M3 alone. The attributes for

M3 were obtained from seismic data in time domain (both conventional and acoustic inverted seismic data), while for M2 and M4 a depth domain acoustic inverted data was used. One issue on this methodology is the reduced number of wells. Although this obviously cannot be solved excepting by more drilling, a check for the correlation significance was performed by excluding one well at a time and verifying possible significant changes in the correlation coefficient obtained ('blind test').

The correlations were obtained separately for reservoirs 330A, B and C for M2 and M4. On M3 study, 330 was considered as a single unit.

The petrophysical parameters of interest were effective porosity (ϕ), net-to-gross ratio (NTG) and horizontal permeability (k_h).

At M2 and M3, 20 attributes were tested on five wells for 330A; correlations were found between the second (linear) term of the polynomial that reconstructs the seismic trace (C_1) and k_h (100 %), the minimum amplitude inside the reservoir and NTG (98.6 %) and integrated cosine of phase and ϕ (88.8 %). 330B had 21 attributes tested on six wells, giving as results correlations between amplitude difference and k_h (81.6 %), the first (bias) polynomial term (C_0) and NTG (80.7 %) and integrated reflection strength and ϕ (86.1 %). For 330C, from 28 attributes analyzed at only three wells, reflection strength was selected for all petrophysical parameters, with correlation of 97.3 % with k_h , 99.9 % with NTG and 98.7 % with ϕ .

For M3, five wells were used; k_h had 92.8 % with the tenth polynomial term (C_{10}), NTG 93.6 % against C_5 and ϕ 89.7 % with maximum amplitude.

The use of seismic attributes – although causing a 33.10^6 Mm³ oil volume reduction in compartments of wells A and G – gave a geologic model much more realistic than before for both M2 and M4 (Fig. 6) and M3.

Neural network for reservoir characterization

Oil-type prediction was very successful using neural networks for well F; three seismic attributes and a back-propagation (supervised) method were used (Rodriguez-Suarez, 2002). The same approach was tested on M2 and M4, but the results weren't as satisfactory. Although some results seem to have geological meaning, in general this is not true, and more studies are necessary.

For example, when M2 and M4 are divided in five (or six) compartments, the results are meaningless. It was observed that the use of a higher number of classes (from two to six) make the results less geologically plausible. The possible reasons for this are being currently analyzed; among the possibilities to be considered (and verified) are presence of gas on well B (causing strong amplitude anomalies), OWC close to the reservoir top for well E and poor definition of 330A/B boundary and/or reservoir bottom (due to polarity changes).

The above conclusions do not stand for 330C, where results with geological meaning were obtained.

Conclusions

Seismic attributes (including terms of a polynomial which reconstruct seismic traces) were used on reservoir characterization at Roncador, resulting on geological model and fluid flow simulator with much more geologic sense when compared to a model based on well data only. Appraisal wells, drilled based on interpretation of acoustic inverted seismic data converted to depth via an image-ray method, were successful. Additional works are necessary on neural network analysis for reservoir characterization.

Acknowledgments

To PETROBRAS, for permission to present this work. To the processing group of PETROBRAS/UN-RIO and Dr. Guenther Schwedersky Neto for performing seismic inversion and time to depth conversion. To Mr. Mauro Mihaguti and Dr. Carlos E. Theodoro for text review and suggestions. To Ms. Monica Rebelo for figures edition.

References

Filpo, E. and Zago, N., 2001, *Updating the velocity field in true-amplitude zero-offset time migration*, 2nd Wave Technology Workshop on Seismic True Amplitudes, Karlsruhe, Germany.

Moraes, J.A., 2000, *Reflection impedance sections construction using zero offset migration*, MSc thesis, UNICAMP, Brazil (in Portuguese).

Rodriguez-Suarez, C., 2002, *Seismic interpretation of an ultra deepwater field – a case study from Roncador, Brazil*, 64th Mtg. EAGE. Session: P076.

Rosa, A.L.R. and Tassini, J., 1995, *Introduction to seismic trace inversion*, PETROBRAS internal course notes.

Rosa, A.L.R., Cunha, C.A, Pedrosa, I., Panetta, J., Sinedino, S. and Braga, V., 1999, *Two-pass 3-D prestack time-migration*, 6th Int. Cong. SBGf, Rio, paper 103.

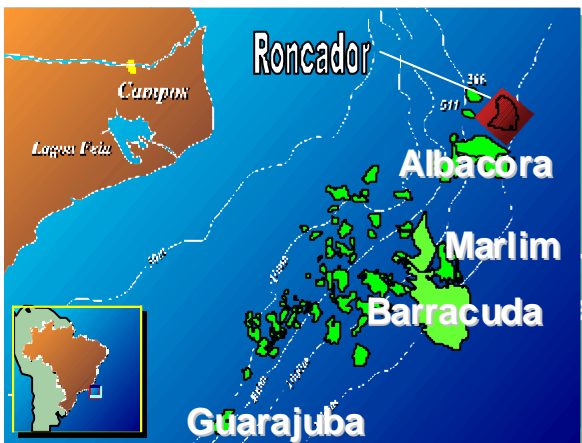


Fig. 1: Campos basin and Roncador field

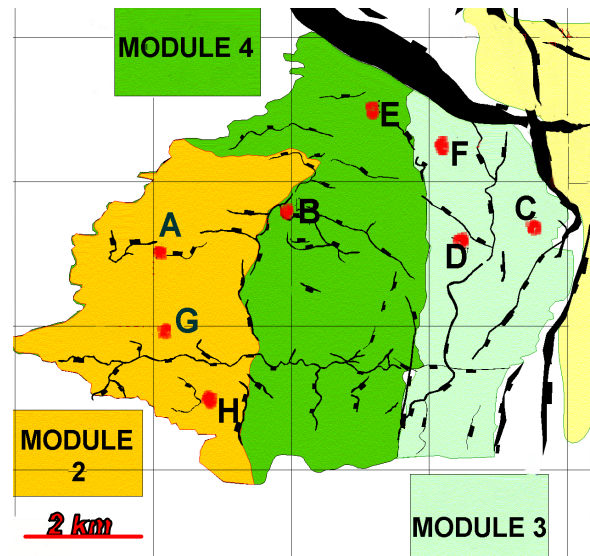


Fig. 2: Module division at Roncador footwall. M2 and M4 have 18° API oil and M3 22°.

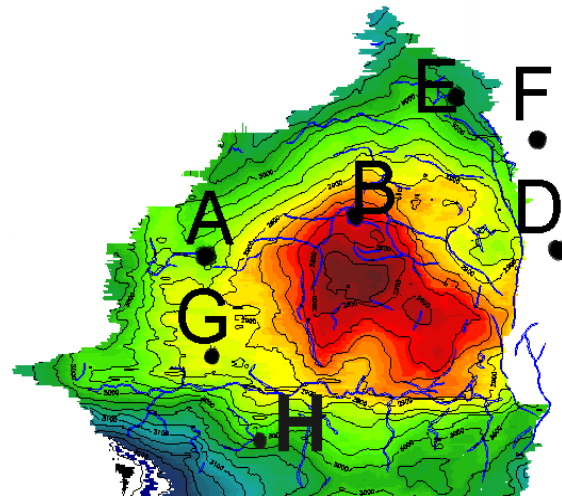


Fig. 5: Structural map of reservoir top at M2 and M4, showing N-S and E-W trends and ring-type pattern around apex.

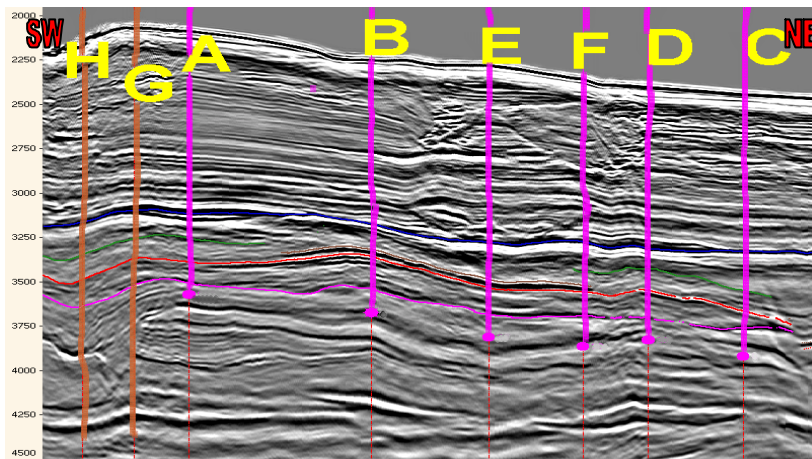


Fig. 3: Seismic section in time, showing smooth dip E-NE. Reservoir top and bottom are red and pink surfaces, respectively.

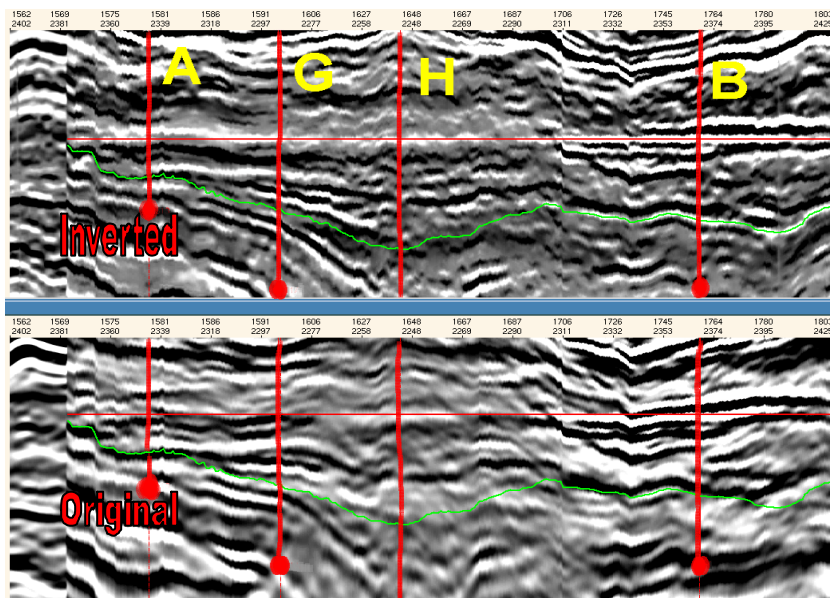


Fig. 4: Depth seismic section horizontalized at reservoir top, showing original (bottom) and inverted seismic data.

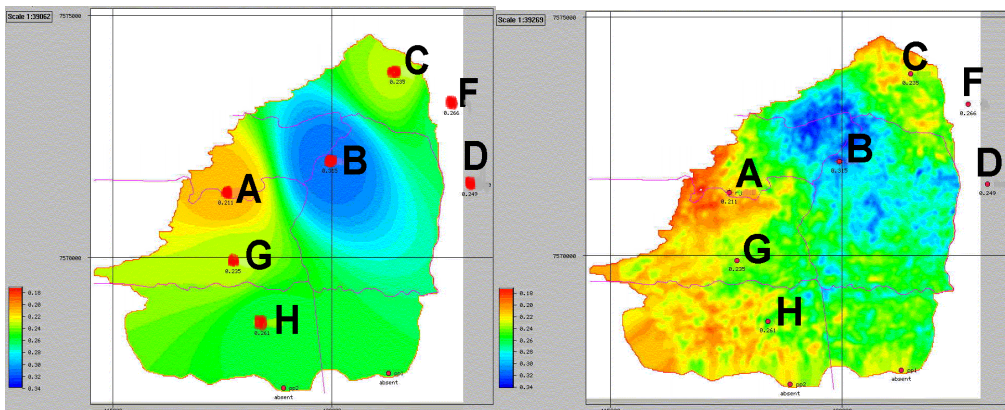


Fig. 6: Comparison of porosity map without (left) and with use of seismic attributes for M2 and M4.